

BAMBOO FLOUR/PETG COMPOSITES: COMPATIBILIZING EFFECT OF POLY(METHYL METHACRYLATE) GRAFTED ONTO BAMBOO FLOUR

FANGBING YU,^{***} QIUNING WU,^{*} JINGBING CHEN,^{*} JIANBIN SONG^{*} and WENBIN YANG^{*}

^{*}College of Material Engineering, Fujian Agriculture and Forestry University,
Fuzhou 350002, China

^{**}National Center for Quality Supervision and Testing of Wood-Based Panel and Chemical Forest Products,
Sanming 365000, China

✉ Corresponding authors: Wenbin Yang, fafuywb@163.com
Jianbin Song, jianbin1102@163.com

Received December 21, 2017

In order to improve the interfacial interaction between poly(ethylene glycol-co-cyclohexane-1,4-dimethanol terephthalate) (PETG) and bamboo flour, the surface of bamboo flour (BF) was modified with methyl methacrylate (MMA) using the electron transfer (AGET) atom transfer radical polymerization (ATRP) method. The grafted BF was characterized by Fourier transform infrared spectroscopy (FTIR), scanning electron microscopy (SEM) and thermogravimetric analysis. The MMA groups had been successfully grafted onto the BF surface and the contact angle of the grafted BF was as high as 130°. The maximum flexural strength was determined to be 72 MPa for the composite containing 20 wt% modified BF, which was higher than that of the composite containing 20 wt% original BF (62 MPa). Also, the decrease in loss factor indicated that the grafting modification improved the compatibility between PETG and BF, and this conclusion was also confirmed by SEM. The results have great practical significance for the application of PETG/BF composites.

Keywords: bamboo flour, AGET ATRP, PETG, mechanical properties

INTRODUCTION

An efficient use of wood biomass as a sustainable carbon-neutral resource is essential for constructing a recycling society, and the demand for wood biomass has increased gradually. In line with this development, bio-based wood/polymer composites (WPC) have received considerable attention due to their advantages of low processing cost, durability, biodegradability, high modulus of elasticity (MOE), 3-D-formability and recyclability.¹⁻⁵ However, large differences in surface energy between the hydrophilic wood and the hydrophobic polymer matrix often lead to poor interfacial adhesion and therefore to poor ability to transfer stress between the matrix and the reinforcing fibers.⁶ In order to achieve better performance, the interfacial interaction of these composites should be improved. So far, a wide

variety of surface modification techniques based on physical or chemical means have been developed by the industry and academia.^{2-5,7-13} Among these methods, the main one is to add coupling agents or compatibilizers into the polymer matrix. For polyolefin composites, the most often used compatibilizers are maleic anhydride-grafted PE or PP.^{11,14,15} The anhydride groups can react chemically with the hydroxyl groups of wood fibers or flour, also, the other end of the copolymer entangles with the polymer matrix. However, often such modification does not solve all the problems of wood-polymer composites, such as aggregation or water absorption of wood fiber or flour. Based on that, the modification of cellulose or wood flour by graft copolymerization provides a significant

route to increase dispersion of the particles, reduce water sorption, or improve composite properties. Over the past two decades, many techniques, such as free radical polymerization,¹⁶⁻²⁰ ring-opening polymerization,^{21,22} single-electron-transfer living radical polymerization (SET-LRP),^{23,24} nitroxide-mediated polymerization (NMP),^{25,26} reversible addition-fragmentation chain transfer (RAFT) polymerization^{27,28} and atom transfer radical polymerization (ATRP),²⁹⁻³⁴ have been applied to cellulose grafting. Among these techniques, ATRP, proposed by Matyjaszewski³⁵ and Sawamoto,³⁶ is one of the most powerful and versatile techniques. It has been widely studied and applied because it possesses many unique advantages, and could be used as a versatile tool to create polymers with narrow polydispersity, well-controlled molecular weight, various architectures and functionalities.³⁷

However, normal ATRP has some disadvantages, for example, the catalyst used is sensitive to oxygen or other oxidizers.³⁸ In order to overcome the drawbacks of normal ATRP, more recently, an improved ATRP technique, activator generated by electron transfer atom transfer radical polymerization (AGET ATRP) has been developed by Matyjaszewski's group.³⁹⁻⁴¹ In this polymerization system, the activating catalyst species Cu(I) is formed by the reduction of the air-stable Cu(II) species *in situ* with the reducing agent, such as ascorbic acid (VC). Thus, AGET ATRP has the advantages of facile preparation, storage and handling of ATRP catalysts.⁴² Since its development in 2005, AGET ATRP has become one of the most powerful, versatile, simple and inexpensive methods in the living/controlled free radical polymerization, and successfully applied to polymer synthesis.⁴³ However, to the best of our knowledge, studies about grafting monomers onto bamboo flour *via* the AGET ATRP method have been less reported.

Bamboo, an important renewable resource, grows faster than almost all the trees on the earth. It can reach the maximum height of 15~30 m within 2 to 4 months and full-stand maturity within 3 to 5 years.⁴⁴ Furthermore, the overall mechanical properties of bamboo are comparable to those of wood, and thus these advantages make bamboo a highly competitive natural material for reinforcing polymer composites. Recently, bamboo fiber or flour has been widely used as

reinforcement of PE,^{45,46} PVC^{47,48} and PP.^{49,50} Poly(ethylene glycol-co-cyclohexane-1,4-dimethanol terephthalate) (PETG) is an amorphous polyester with excellent impact strength and processing performance. To the best of our knowledge, few attempts have been made to develop PETG/bamboo flour composites.

In order to overcome the hydrophilicity of bamboo flour and improve the adhesion between PETG and bamboo flour, in this work, PMMA was successfully grafted to the surface of bamboo flour using the AGET ATRP method. Concurrently, the mechanical properties and morphology of the BF/PETG composites were investigated. In addition, the effect of the grafted bamboo flour on the dynamic mechanical properties of the BF/PETG composites was also studied. Meaningful results were expected, enabling further research on bamboo/plastic composites.

EXPERIMENTAL

Materials

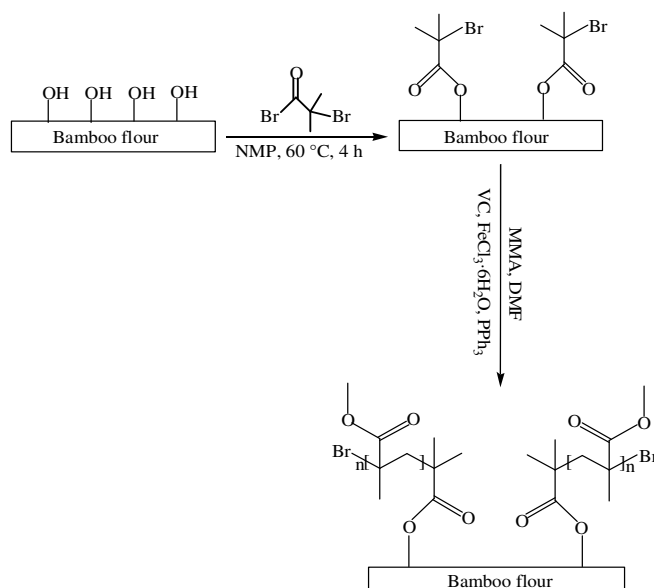
Bamboo flour (BF), with an average size of 60-80 mesh, was supplied by Linan Mingzhu Bamboo & Wood Powder Co., Ltd. (Zhejiang, China). Before use, BF was dried in an oven at 105 °C for 24 h to remove water. Poly(ethylene glycol-co-cyclohexane-1,4-dimethanol terephthalate) (PETG) was bought from Eastman Chemical Co., Ltd. (Guangdong, China). Tetrahydrofuran (THF) (AR), iron (III) chloride hexahydrate (FeCl₃·6H₂O) (>99%), N-methyl pyrrolidone (NMP, 99%), triphenyl phosphine (PPh₃) (AR) and L-ascorbic acid (>99.7%) were purchased from Tianjin Fuchen Chemical Reagent Factory. 2-Bromoisobutryl bromide (BIBB, 98%) was purchased from Chengdu Best Reagent Co., Ltd. The monomer, methyl methacrylate (MMA, 99%), was also purchased from Tianjin Fuchen Chemical Reagent Factory. MMA was washed with an aqueous solution of sodium hydroxide (5 wt%) three times, followed by deionized water until neutralization, and then dried over anhydrous sodium sulfate, distilled under reduced pressure and stored in an air-free flask in the freezer. N,N-dimethylformamide (DMF) (AR) and all the other reagent grade chemicals were purchased from Shanghai Sinopharm Chemical Reagent Co., Ltd. and used as received, unless mentioned otherwise.

Immobilization of initiator on BF surface

The procedure of initiator immobilization on the BF surface was similar to that reported by Liu *et al.*⁵¹ The dried BF specimen was placed into a 250 mL round-bottomed flask, equipped with a pressure

dropping funnel and an electric stirring bar; 40 mL NMP was added to it and then the flask was placed in an ice bath and gently stirred. When the above mixture was cooled to 0 °C, a solution of BIBB (5 mL) in NMP (5 mL) was added dropwise into the mixture under nitrogen atmosphere. After that, the flask was heated to

60 °C using a water bath and held at 60 °C for 4 h. Subsequently, the BF specimen was taken out from the flask and extracted for another 8 h by Soxhlet extraction with ethanol, and then dried in a vacuum oven at 50 °C for 24 h.



Scheme 1: ATRP of MMA from bamboo flour surface

The surface-initiated AGET ATRP of MMA on the BF-Br surfaces was accomplished by the following procedure: MMA (10 mL, 28.4 mmol), BF-Br (0.25 g), $\text{FeCl}_3 \cdot 6\text{H}_2\text{O}$ (0.084 g, 0.0057 mmol), PPh_3 (5.9 μL , 0.0284 mmol), Vc (0.218 g, 0.0057 mmol) and DMF (5 mL) were added to a 50 mL round-bottomed flask. Firstly, the mixture was bubbled with nitrogen for 5 min, and then it was transferred to a water bath (65 °C). After a predetermined time, the flask was cooled with ice water. The grafted sample was thoroughly rinsed with ethanol, acetone, THF and followed by Soxhlet extraction with THF for another 48 h to completely remove any unreacted and unbounded materials.³¹ At last, the sample was dried in a vacuum oven at 50 °C for 24 h. The whole process is shown in Scheme 1.

Preparation of composites

BF was dried at 105 °C for 24 h to remove moisture and then stored in sealed containers. In order to study the effect of modification of BF on the properties of the BF/PETG composites, a series of composites with BF/PETG of 20/80, 30/70 and 50/50 were prepared. The blending process was performed using a HAAKE MiniLab II internal mixer at 190 °C for 6 min and 40 rpm. Afterwards, the compounded composite was compressed into 2 mm thick plates,

using an oil-heated press at 190 °C for 10 min and a pressure of 8 MPa.

Characterization

FTIR spectroscopy

The BF surface was characterized by Fourier transform infrared spectroscopy (Thermo Scientific Nicolet 380, USA). The data were collected in the range of 4000-400 cm^{-1} , using 32 scans at 4 cm^{-1} resolution.

Thermogravimetric analysis

The thermogravimetric analysis (TGA) of BF was carried out using a STA449 F3 Jupiter thermogravimetric analyzer from NETZSCH Instruments. Alumina ceramic pans were used. The sample was heated from room temperature to 700 °C at a rate of 10 °C/min under nitrogen atmosphere.

X-ray diffraction analysis

X-ray diffraction (XRD) tests were performed by an X-ray diffractometer (X'Pert Pro MDP, Philips, Netherlands) with Ni-filtered $\text{Co-K}\alpha$ radiation at 40 kV and 30 mA. The XRD data were gathered in the range of $2\theta = 5^\circ \sim 60^\circ$.

Water contact angle analysis

Water contact angle (WCA) measurements were carried out in the air with a water droplet (static sessile drop method) with an OCA15EC contact angle analyzer produced by Dataphysics (Germany) to evaluate the surface properties of modified BF.

SEM analysis

Surface morphology was characterized using a Philips-FEI XL30 WESM-TEP microscope (Netherlands), operating at an accelerating voltage of 20 kV. Prior to observation, the BF and composite fracture surfaces were sputtered with a layer of gold to avoid electrical charging during examination.

Mechanical tests

Flexural properties were tested with a CMT-6104 universal testing machine (Shenzhen Sans Material Test Instrument Co., Ltd., China) and the cross-head speed adopted was 5 mm/min. The sample dimensions were controlled to be 50 mm × 6 mm × 2 mm. All the data reported here represent the average of the results for at least five specimens.

Dynamic mechanical analysis

Dynamic mechanical analysis (DMA) was performed using DMA 242D (Netzsch, Germany) with a three-point bending mode and a frequency of 2 Hz. The specimens were 45 mm × 6 mm × 2 mm and were heated from 25 °C to 150 °C at a heating rate of 5 °C/min.

RESULTS AND DISCUSSION**Polymer grafting****FTIR analysis**

Figure 1 shows the typical FTIR spectra of PMMA, pristine BF and PMMA-grafted BF during different time periods. PMMA exhibits the

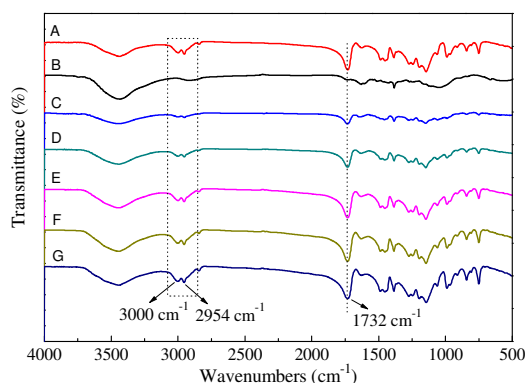


Figure 1: FTIR spectra of PMMA (A), pristine BF (B), BF-g-PMMA 2 h (C), BF-g-PMMA 3 h (D), BF-g-PMMA 4 h (E), BF-g-PMMA 5 h (F) and BF-g-PMMA 6 h (G)

two absorption peaks at 3000 cm^{-1} and 2954 cm^{-1} , corresponding to the stretching vibration of -CH-. The peak at 1732 cm^{-1} is attributed to the stretching vibration of the ester carbonyl group, and this peak intensity increases as the reaction time lengthens, indicating successful growth of the surface-grafted polymer *via* the AGET ATRP method.

Thermogravimetric analysis

The thermal behaviors of pristine BF and grafted BF are studied as a function of percentage weight loss with increasing temperature. Figure 2 shows the TGA curves of pristine BF and grafted BF. From the TGA of pristine BF, the first weight loss of 4.04% is due to loss of absorbed and bound water. Thereafter, the decomposition of BF onsets at 206 °C and continues up to 680 °C. The results confirm that there is 99.07% weight loss due to the degradation of macromolecular chains. The TGA of the grafted product is different. It is observed that grafted BF has better thermal stability than pristine BF and BF-Br. The decomposition process of grafted BF includes two steps. The initial decomposition temperature is determined at 210 °C and the final decomposition temperature appears at 430 °C. From the TGA of PMMA-grafted BF, it can also be seen that the percentage of the first weight loss gradually decreases with the increase of the reaction time. It illustrates that the thermal properties of the PMMA-grafted BF are significantly affected by the amount of polymer grafted onto the BF surface.

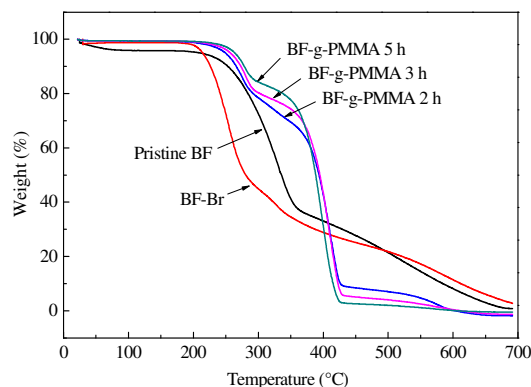


Figure 2: TGA curves of BF before and after grafting

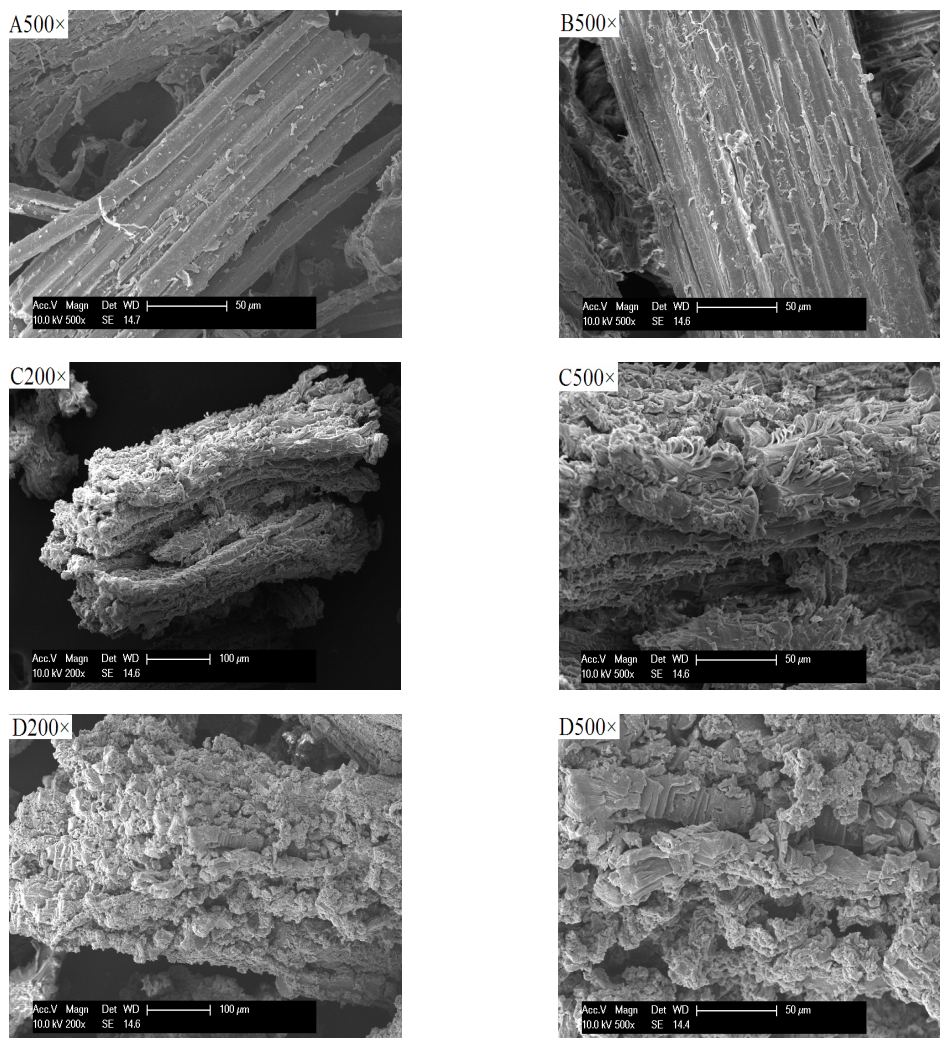


Figure 3: SEM images of pristine BF (A), BF-Br (B), BF-g-PMMA 2 h (C) and BF-g-PMMA 5 h (D)

EAEM analysis

The effects of graft polymerization on the surface morphology of the BF were investigated by ESEM. Figure 3 shows the surface morphology of the pristine and grafted BF. It can be seen that the pristine BF exhibits a smooth surface without any material attached to the surface. After modification, the surface of the BF becomes extremely rough because of the grafting of PMMA onto the BF. This result is consistent with other published works, in which rough surfaces were found after graft polymerization.^{52,53}

XRD analysis

X-ray diffraction patterns of pristine BF, BF-Br, BF-g-PMMA 2 h, BF-g-PMMA 3 h,

BF-g-PMMA 5 h and PMMA are shown in Figure 4. From the comparison of pristine BF and BF-Br, the characteristic diffraction peaks of the pristine BF at $2\theta = 18^\circ$ and 25.5° are stronger than those of BF-Br. This indicates that the esterification reaction between the initiator (BIBB) and the BF surface resulted in a destructive effect on the microcrystal structure of BF cellulose.⁵⁴ Compared with the pristine BF, the characteristic diffraction peaks at $2\theta = 18^\circ$ and 25.5° almost disappeared in the patterns of all the grafted substrates. In addition, a new peak appeared at $2\theta = 15^\circ$, which has been reported by Peña and co-workers.⁵⁵ Therefore, it is reasonable to assume that the monomers are grafted onto the BF surface.

Wettability studies

Figure 5 shows optical photos of water contact angles on BF-Br and BF-g-PMMA. The pristine BF surface is hydrophilic because of the presence of numerous hydroxyl groups, the water droplet spread quickly when it contacted the surface of pristine bamboo flour, so the WCA measurement could not be performed at all. From Figure 5 (A), it is observed that the hydrophobicity of BF surface is enhanced significantly after esterification. The water contact angle of BF-Br is 89.4° . Moreover, after the AGET ATRP reactions, the water contact angles of the grafted surfaces drastically increased to 130° for the sample subjected to reaction during 5 h, which indicated that the BF surface had become more hydrophobic.

Microscopy of composite fracture surfaces

Figure 6 corresponds to the fracture micrographs of unmodified and modified BF/PETG composites. It is easily recognized in Figure 6 (A) that unmodified BF performs very poor interface bonding with the PETG matrix.

Interfacial debonding is obviously observed and little plastic matrix adhering onto the BF surface is found. However, after grafting modification, the interfacial properties of the composites were obviously improved, which can be observed in Figure 6 (B). The BF is coated by the polymer matrix, and the interface of the two phases is not apparent. This suggests that the AGET ATRP method could effectively improve the interfacial compatibility between BF and PETG, and this result is also verified by the mechanical properties exhibited in Figure 7.

Mechanical properties**Flexural properties of composites**

Figure 7 shows the flexural properties of BF/PETG composites. When BF is compounded with PETG directly, the poor adhesion properties between BF and PETG lead to poor flexural strength. Compared with the unmodified BF/PETG composites, the flexural strength of the modified BF/PETG composites is significantly improved.

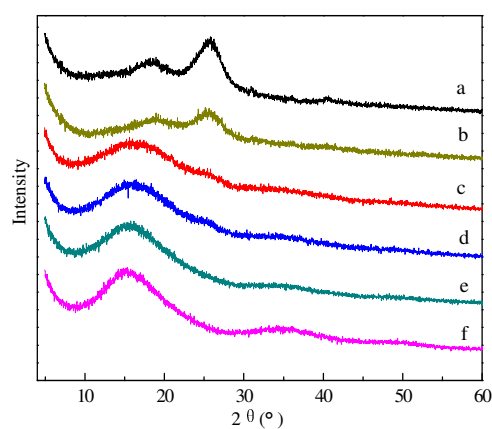


Figure 4: XRD patterns of pristine BF (a), BF-Br (b), BF-g-PMMA 2 h (c), BF-g-PMMA 3 h (d), BF-g-PMMA 5 h (e) and PMMA (f)

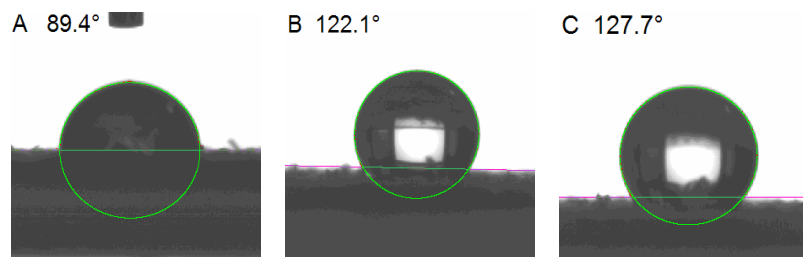


Figure 5: Water contact angles of BF-Br (A), BF-g-PMMA 2 h (B) and BF-g-PMMA 5 h (C)

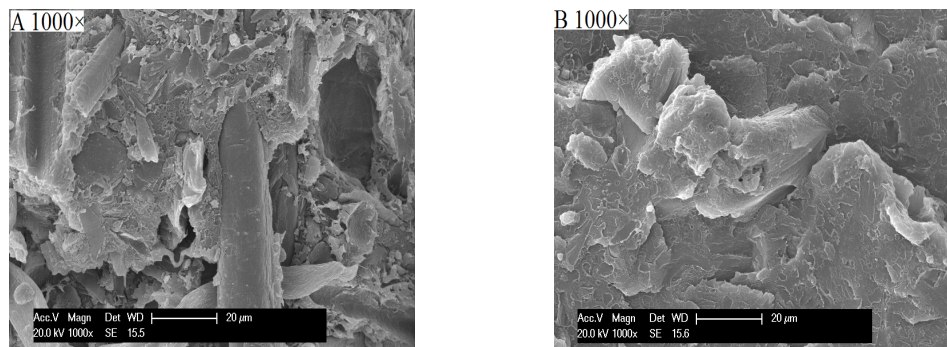


Figure 6: Scanning electron micrographs of cryofractured surface of 30 wt% BF/PETG composites: pristine BF (A) and grafted BF (B)

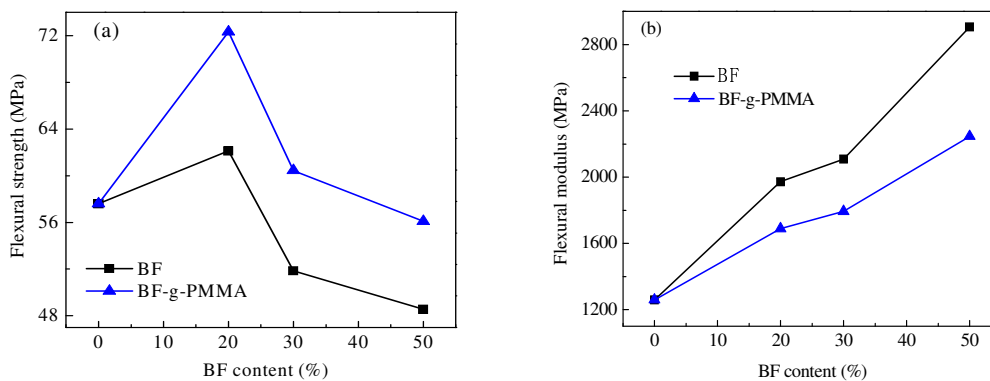


Figure 7: Flexural strength *versus* content of BF in composites

It indicates that the grafting modification of BF by coating it with a layer of PMMA could improve the internal bond strength and reduce the interface defects between BF and PETG. Taking into account the BF content, the composites with higher BF content (30 wt%) exhibit a lower flexural strength than those with lower BF content (20 wt%). The reason may be that increasing the BF content automatically leads to BF aggregation and produces more interfacial defects, which results in poor stress transfer between the polymer matrix and BF.⁵⁶

Dynamic mechanical properties

DMA is a useful technique to study the dynamic mechanical behavior, molecular relaxations and interactions taking place in the produced materials at varying temperature.⁴⁵ Storage modulus (E') is associated with the elastic response of the composite and could be used to characterize the material stiffness, while the loss modulus (E'') represents the viscous part of the sample. The ratio of E'' to E' is defined as the loss factor ($\tan\delta$), and a composite with a higher $\tan\delta$

suggests that more heat was produced and more deformation could not be recovered when the outside force was removed. From another point of view, it also indicates that the inner friction force was enhanced.

In order to study the effect of grafting modification of bamboo flour on molecular motion, the dynamical mechanical properties of the composites containing 30 wt% and 50 wt% bamboo flour were assessed at a frequency of 2 Hz. The E' and $\tan\delta$ of the BF/PETG composites as a function of temperature are shown in Figure 8.

Figure 8 (a, b) presents the corresponding E' curves of PETG and the composites. As expected, the magnitude of E' is remarkably increased with the incorporation of rigid BF into PETG, which is indicative of enhancing stiffness.^{2,45} Among these composites, the composite with unmodified BF exhibits a higher E' value than the modified composite over the entire experimental temperature range, and such a trend is in agreement with that obtained for the static modulus (Fig. 7 (b)).

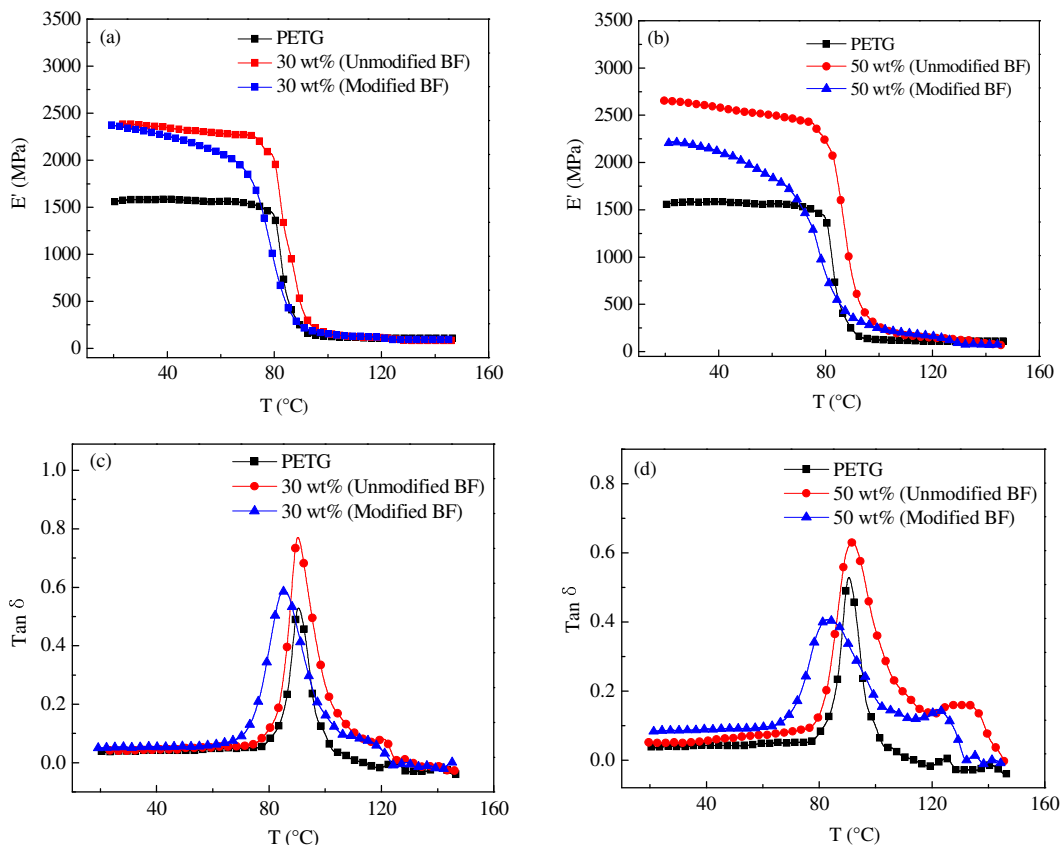


Figure 8: Variation in storage modulus and loss tangent as a function of temperature for BF/PETG composites

Figure 8 (c, d) shows the corresponding $\tan\delta$ curves of PETG and its composites. As shown in the figures, a big relaxation process is found at 90 °C for PETG, and this loss peak is attributed to the glass transition temperature (T_g) of PETG. When PETG is blended with unmodified BF, this loss peak position does not change, but a decrease in magnitude is observed, suggesting the inner friction force in the unmodified BF/PETG composite became larger than in the neat PETG. However, when PETG is added to modified BF, the loss peak position shifts towards low temperature, suggesting an enhanced moving ability of PETG. The reason is that PMMA on the BF surface can increase the distance between BF and PETG, and as a result, PETG molecules move more easily. The changes in T_g show that BF grafting with PMMA can effectively improve the interfacial compatibility between BF and PETG. At the same time, the $\tan\delta$ of the modified BF/PETG composite is lower than that of the unmodified BF/PETG composite, indicating that more deformation could recover when the outside

force was removed, *i.e.* the elastic part increased, and this is related to the increase in the molecular movement ability of PETG.

CONCLUSION

Graft polymerization of MMA onto the surface of BF by electron transfer (AGET) atom transfer radical polymerization (ATRP) is found to be an efficient and convenient method for modifying the physicochemical properties of BF and improving the interfacial adhesion between PETG and BF. This method has successfully turned hydrophilic BF into hydrophobic BF as the reaction time surpassed 2 h. Compared with pristine BF, after grafting the bamboo flour is engulfed in the matrix. The strong interlocking of the BF-matrix bonding, which is indicative of improved interfacial interaction, could be observed by SEM.

ACKNOWLEDGEMENTS: This work was financially supported by the Program for National Natural Science Foundation of China (No.

31170535 and 30771683) and Postdoctoral Science Foundation of China (No. 2016T90150 and 2014M560138).

REFERENCES

- ¹ H. Jeske, A. Schirp and F. Cornelius, *Thermochim. Acta*, **543**, 165 (2012).
- ² T. F. Qin, L. H. Huang and G. Y. Li, *J. For. Res.*, **16**, 241 (2005).
- ³ M. S. Islam, S. Hamdan, M. Hasan, A. S. Ahmed and M. R. Rahman, *Int. Biodeter. Biodegrad.*, **72**, 108 (2012).
- ⁴ J. Y. Kim, J. H. Peck, S. H. Hwang, J. Hong, S. C. Hong *et al.*, *J. Appl. Polym. Sci.*, **108**, 2654 (2008).
- ⁵ Y. J. Xie, C. A. S. Hill, Z. F. Xiao, H. Militz and C. Mai, *Composites: Part A*, **41**, 806 (2010).
- ⁶ H. C. Yi, S. Lee and T. Jie, *J. Vinyl. Addit. Technol.*, **14**, 211 (2008).
- ⁷ G. Haddou, J. Dandurand, E. Dantras, H. Maiduc, H. Thai *et al.*, *J. Therm. Anal. Calorim.*, **129**, 1463 (2017).
- ⁸ E. H. Sun, F. W. Sun, Z. Zhang and Y. D. Dong, *Surf. Interface Anal.*, **48**, 64 (2016).
- ⁹ G. Haddou, J. Dandurand, E. Dantras, H. Maiduc, H. Thai *et al.*, *J. Therm. Anal. Calorim.*, **124**, 701 (2016).
- ¹⁰ O. Nozari, M. Madanipour, M. Farsi and A. Tabei, *Cellulose Chem. Technol.*, **47**, 295 (2013).
- ¹¹ L. Dányádi, J. Móczó and B. Pukánszky, *Composites: Part A*, **41**, 199 (2010).
- ¹² S. S. Chauhan, P. Aggarwal, G. S. Venkatesh and R. M. Abhilash, *Int. J. Plast. Technol.*, **22**, 85 (2018).
- ¹³ W. P. Zhang, X. Yao, S. Khanal and S. A. Xu, *Constr. Build. Mater.*, **186**, 1220 (2018).
- ¹⁴ X. Y. Chen, Q. P. Guo and Y. L. Mi, *J. Appl. Polym. Sci.*, **69**, 1891 (1998).
- ¹⁵ Z. Dominkovics, L. Dányádi and B. Pukánszky, *Composites: Part A*, **38**, 1893 (2007).
- ¹⁶ K. C. Gupta and K. Khandekar, *J. Appl. Polym. Sci.*, **101**, 2546 (2006).
- ¹⁷ F. E. Okieimen, *J. Appl. Polym. Sci.*, **89**, 913 (2003).
- ¹⁸ F. Khan, *Macromol. Biosci.*, **5**, 78 (2005).
- ¹⁹ A. Pourjavadi and G. R. Mahdavinia, *J. Polym. Mater.*, **22**, 235 (2005).
- ²⁰ P. Ghosh and D. Dev, *Eur. Polym. J.*, **32**, 165 (1996).
- ²¹ Y. Teramoto, S. Ama, T. Higeshiro and Y. Nishio, *Macromol. Chem. Phys.*, **205**, 1904 (2004).
- ²² L. Carlsson, T. Ingverud, H. Blomberg and A. Carlmark, *Cellulose*, **22**, 1063 (2015).
- ²³ B. M. Rosen and V. Percec, *Chem. Rev.*, **109**, 5069 (2009).
- ²⁴ N. H. Nguyen and V. Percec, *J. Polym. Sci.: Part A*, **48**, 5109 (2010).
- ²⁵ W. H. Daly, T. S. Evenson, S. T. Iacono and R. W. Jones, *Macromol. Symp.*, **174**, 155 (2001).
- ²⁶ C. J. Hawker, A. W. Bosman and E. Harth, *Chem. Rev.*, **101**, 3661 (2001).
- ²⁷ G. Moad, E. Rizzardo and S. H. Thang, *Polymer*, **49**, 1079 (2008).
- ²⁸ S. Perrier, P. Takolpuckdee, J. Westwood and D. M. Lewis, *Macromolecules*, **37**, 2709 (2004).
- ²⁹ A. Carlmark and E. Malmström, *J. Am. Chem. Soc.*, **124**, 900 (2002).
- ³⁰ J. Lindqvist, D. Nyström, E. Östmark, P. Antoni, A. Carlmark *et al.*, *Biomacromolecules*, **9**, 2139 (2008).
- ³¹ F. B. Yu, W. B. Yang, J. B. Song, Q. N. Wu and L. H. Chen, *Wood Sci. Technol.*, **48**, 289 (2014).
- ³² X. Q. Zhang, J. L. Zhang, L. L. Dong, S. X. Ren, Q. L. Wu *et al.*, *Cellulose*, **24**, 4189 (2017).
- ³³ G. Morandi and W. Thielemans, *Polym. Chem.*, **3**, 1402 (2012).
- ³⁴ B. Volynets, H. Nakhoda, M. A. Ghalia and Y. Dahman, *Fibers Polym.*, **18**, 859 (2017).
- ³⁵ J. S. Wang and K. Matyjaszewski, *J. Am. Chem. Soc.*, **117**, 5614 (1995).
- ³⁶ M. Kato, M. Kamigaito, M. Sawamoto and T. Higashimura, *Macromolecules*, **28**, 1721 (1995).
- ³⁷ T. L. Xing, W. L. Hu, S. W. Li and G. Q. Chen, *Appl. Surf. Sci.*, **258**, 3208 (2012).
- ³⁸ G. Moineau, P. Dubois, R. Jérôme, T. Senninger and P. Teyssié, *Macromolecules*, **31**, 545 (1998).
- ³⁹ K. Min, H. F. Gao and K. Matyjaszewski, *J. Am. Chem. Soc.*, **127**, 3825 (2005).
- ⁴⁰ W. Jakubowski, K. Min and K. Matyjaszewski, *Macromolecules*, **39**, 39 (2006).
- ⁴¹ K. Min, W. Jakubowski and K. Matyjaszewski, *Macromol. Rapid Commun.*, **27**, 594 (2006).
- ⁴² F. Tang, L. F. Zhang, J. Zhu, Z. P. Cheng and X. L. Zhu, *Ind. Eng. Chem. Res.*, **48**, 6216 (2009).
- ⁴³ Y. Sun and W. Q. Liu, *Polym. Bull.*, **68**, 1815 (2012).
- ⁴⁴ W. Liese and F. R. G. Hamburg, *Wood Sci. Technol.*, **21**, 189 (1987).
- ⁴⁵ H. Liu, Q. Wu, G. Han, F. Yao, Y. Kojima *et al.*, *Composites: Part A*, **39**, 1891 (2008).
- ⁴⁶ G. P. Han and W. L. Cheng, *Adv. Mater. Res.*, **113/114**, 2349 (2010).
- ⁴⁷ X. C. Ge, X. H. Li and Y. Z. Meng, *J. Appl. Polym. Sci.*, **93**, 1804 (2004).
- ⁴⁸ H. Wang, R. Chang, K. C. Sheng, M. Adl and X. Q. Qian, *J. Bionic Eng.*, **5**, 28 (2008).
- ⁴⁹ G. F. Cai, J. K. Wang, Y. N. Nie, X. C. Tian, X. D. Zhu *et al.*, *Polym. Compos.*, **32**, 1945 (2011).
- ⁵⁰ S. K. Chattopadhyay, R. K. Khandal, R. Uppaluri and A. K. Ghoshal, *J. Appl. Polym. Sci.*, **119**, 1619 (2011).
- ⁵¹ Z. T. Liu, C. A. Sun, Z. W. Liu and J. Lu, *J. Appl. Polym. Sci.*, **109**, 2888 (2008).
- ⁵² S. M. Shang, L. Zhu, W. G. Chen, L. M. Yi, D. M. Qi *et al.*, *Fibers Polym.*, **10**, 807 (2009).

⁵³ V. K. Thakur and A. S. Singha, *Int. J. Polym. Anal. Charact.*, **16**, 153 (2011).

⁵⁴ Y. Fu, G. Li, H. P. Yu and Y. X. Liu, *Appl. Surf. Sci.*, **258**, 2529 (2012).

⁵⁵ E. A. E. Peña, N. F. Ramirez, G. L. Barcenás, S. R. V. García, G. A. Villa *et al.*, *Eur. Polym. J.*, **43**, 3963 (2007).

⁵⁶ N. Sombatsompop and K. Chaochanchaikul, *J. Appl. Polym. Sci.*, **96**, 213 (2005).